Available online at www.sciencedirect.com

ScienceDirect

Ceramics International 40 (2014) 4001–4007

CERAMICS INTERNATIONAL

www.elsevier.com/locate/ceramint

Novel synthesis and characterization of silicon carbide nanowires on graphite flakes

Jun Ding, Chengji Deng*, Wenjie Yuan, Hongxi Zhu, Xiaojun Zhang

The State Key Laboratory Breeding Base of Refractories and Ceramics, Wuhan University of Science and Technology, Wuhan 430081, PR China

Received 17 June 2013; received in revised form 11 August 2013; accepted 11 August 2013
Available online 16 August 2013

Abstract

Silicon carbide nanowires were synthesized on the surface of graphite by partially reacting with silicon powders in NaF–NaCl based salt at 1150–1400 °C in argon. The effects of temperature and time of heat treatment as well as Si/graphite ratio on synthesis of SiC nanowires were studied. The results showed that the formation of SiC nanowires started at about 1200 °C, and the amounts of SiC nanowires increased in the resultant powders with increasing temperature. Their morphologies were characterized by scanning electron microscopy and high-resolution transmission electron microscopy. It was found that β-SiC nanowires with diameter of 10–50 nm and various lengths grew along their preferred direction perpendicular to (111). The zeta potential of graphite was also increased after coating with silicon carbide nanowires. SiC nanowires that formed on the graphite surface acted as an anti-oxidant to a certain extent, and they protected the inner graphite from oxidation.

Keywords: Silicon carbide nanowires; Graphite; Molten salt; Synthesis

1. Introduction

Silicon carbide (SiC) nanowires have attracted considerable attention, because of their excellent mechanical and chemical properties, high thermal conductivity, and low thermal expansion coefficient [1–3]. They have been widely applied in the electronics, optics, machinery, advanced engineering, and metallurgy industries [4,5]. To date, several techniques have been explored for the synthesis of one-dimensional (nanotube, nanowire, and nanowhisker) SiC nanostructures [6–12], including laser ablation [13], chemical vapor deposition (CVD) [14], thermal evaporation process with iron as a catalyst [15], vapor–liquid–solid (VLS) growth mechanism [16], vapor–solid (VS) growth mechanism [17], solid–liquid–solid (SLS) growth mechanism [18], *etc*.

Graphite is used as a raw material in the metallurgy, advanced engineering, and coatings industries because of its low thermal expansion coefficient and high thermal conductivity. One of its major features includes non-wettability which is mostly beneficial when used in the context of liquid metal or liquid slag applications [19]. A drawback on the use of graphite is its low oxidation resistance, its increased porosity after drying, and concomitantly reduced mechanical strength. On the other hand, due to the non-wettability of graphite, the resulting castables flow poorly and a considerable water content is required [19]. Such a drawback could be overcome by surface treatment of the graphite which acts as wetting and oxidation resistance between the surrounding environment and the graphite's surface.

At present, graphite is modified by oxides, carbides, or metals, which have better water-wettability and dispersion abilities. Yilmaz et al. [20] used a sol–gel method, to form boehmitic alumina on the graphite's surface, but the treatment initiating this process' required materials is complicated. Chen et al. [4] produced SiC nanowires on a graphite substrate by thermal evaporation of silicon powders at high temperature. Li et al. [21] fabricated nickel-coated graphite nanosheets by an oxidation and reduction process and in MgO–C refractories, often added antioxidants to overcome these inherent drawbacks in the graphite [22]. However, most of the methods require to be manipulated in a complex, expensive and environmentally unfriendly way. Ceramic powders with whisker-, needle-, or plate-like morphologies could be prepared by molten salt synthesis (MSS) [23–27]. It was reported that a titanium carbide coating was synthesized on graphite flakes by MSS [19].

*Corresponding author. Tel.: +86 27 68862041; fax: +86 27 68862085.
E-mail address: cjdeng@wust.edu.cn (C. Deng).

0272-8842/$ - see front matter © 2013 Elsevier Ltd and Techna Group S.r.l. All rights reserved.
http://dx.doi.org/10.1016/j.ceramint.2013.08.051

In this work, molten salt synthesis (MSS) technique was used to synthesize silicon carbide nanowires on graphite flakes. The synthesis mechanism and the change in the structure of silicon carbide nanowires at different temperatures were also studied. Microstructure and growth mechanism of as-prepared SiC nanowires were investigated.

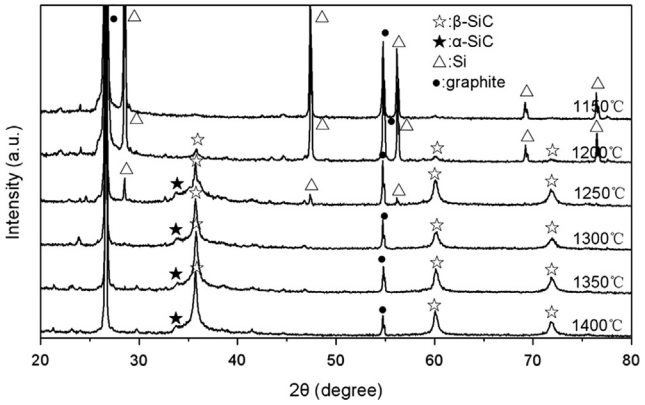

Fig. 1. XRD patterns of samples with a molar ratio of Si/graphite = 1/2 heat-treated for 3 h at different temperatures.

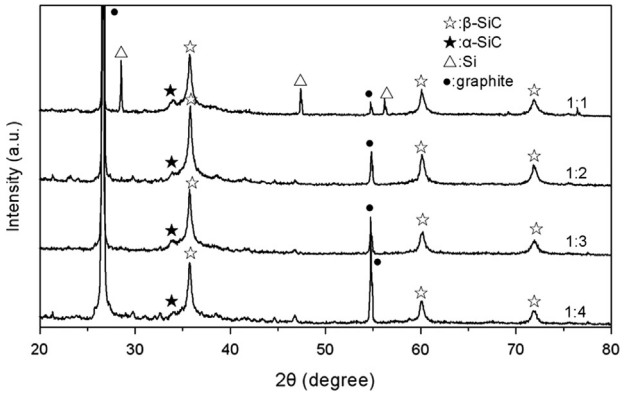

Fig. 2. XRD patterns of samples with a molar ratio of Si/graphite = 1/2 heat-treated at 1400 °C for different times.

2. Experimental materials and procedure

Silicon powder (purity ≥ 99% w/w, particle size ≤ 10 μm), graphite (purity ≥ 97% w/w, particle size 200–300 μm), NaF (purity ≥ 99% w/w) and NaCl (purity ≥ 99% w/w) were used as the raw materials. The molar ratios of Si to graphite were 1:1, 1:2, 1:3, and 1:4, and the weight ratio of NaCl to NaF was 10:1. Mixed salt combined with appropriate amounts of graphite and Si powder was then added. The powder mixture was placed in an alumina crucible and heated for 1, 3, and 5 h at 1150–1400 °C in argon using an alumina-tube furnace. After cooling to room temperature, the solidified mass was repeatedly washed with hot distilled water and filtered several times to remove the residual salt.

Phases in the resultant powders were studied by X-ray diffraction (XRD, Philips, X'Pert Pro), scanning electron microscope (SEM, FEI, Nova 400 Nano) and high-resolution transmission electron microscope (HRTEM, JEOL, JEM-2000F) equipped with energy dispersive X-ray spectroscopy (EDS), respectively. The amount of SiC phase present was calculated using a reference intensity ratio (RIR) from software X'Pert HighScore Plus [28]. The zeta potential of graphite and the treated graphite was determined by a zeta potential analyzer (Zeta Probe, Colloidal Dynamics). The powders and distilled water were confected into a 1% w/w suspension, and then the suspension was subjected to the test for its zeta potential. To elucidate the synthesis and oxidation mechanism of the powders, differential scanning calorimetry (DSC) and thermogravimetric analysis (TGA) were performed at temperatures up to 1200 °C with a heating rate of 10 °C/min in air by a simultaneous thermal analyzer (NETZSCH, STA 449C).

Table 1
Relative content of obtained SiC with a molar ratio of Si/graphite = 1/2 heat-treated for 3 h at different temperatures.

	Temperature of heat treatment (°C)			
	1250	1300	1350	1400
Relative content of SiC (wt%)	2	3	9	12

Table 2
Relative content of obtained SiC with a molar ratio of Si/graphite = 1/2 heat-treated at 1400 °C for different times.

	Heat treatment time (h)		
	1	3	5
Relative content of SiC (wt%)	3	12	9

3. Results and discussion

3.1. Effect of heating temperature and ratio of raw materials on synthesis

The effect of temperature of heat treatment on synthesis of SiC with a molar ratio of Si/graphite of 1:2 is presented in Fig. 1. β-SiC peaks began to appear at 1200 °C and increased in height with increasing temperature from 1200 to 1400 °C. On further increasing the temperature to 1300 °C, Si disappeared, in the meantime β-SiC and graphite phases were obtained. As expected, the amount of β-SiC increased with an increase in the temperature of the heat treatment. In addition, one additional line at $2\theta = 33.82^{\circ}$ in the XRD patterns of SiC samples was detected near the (111) line of the cubic structure of the silicon carbide at $2\theta = 35.64^{\circ}$ which was characteristic of hexagonal polytypes (α-SiC phase) [29]. The results show that the resulting powder products were essentially composed of SiC of cubic type (β-SiC) with a minor amount of α-SiC.

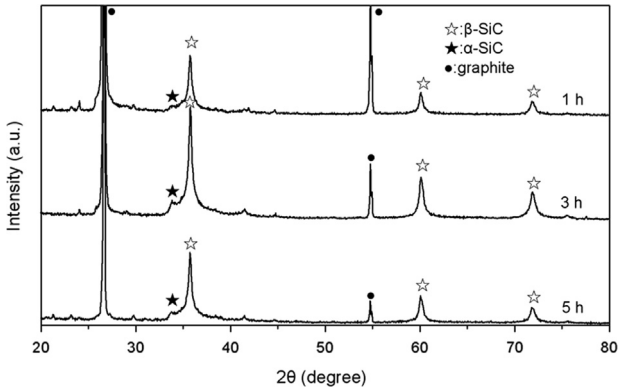

Fig. 3. XRD patterns of samples heat-treated at 1350 °C for 3 h with different Si/graphite ratios.

The β-SiC peaks appeared in the resulting XRD patterns of the heated samples. To illustrate the effect of holding time, XRD patterns of the samples with a molar ratio of Si/graphite of 1:2 heat-treated at 1400 °C for different time periods are shown in Fig. 2. It was seen that holding time of 3 h gave a better conversion efficiency compared to holding times of 1 h or 5 h, as judged by the relative heights of the β-SiC peaks. Also, the additional diffraction peak was detected at $2\theta = 33.82^{\circ}$, which represented stacking faults on the (111) planes in cubic SiC [6]. Shorter holding times were unfavorable to the continuous growth of SiC, while a longer holding time would make molten salts over-volatilize and the liquid phase environment would reduce, both of these effects would be not conducive to the reaction.

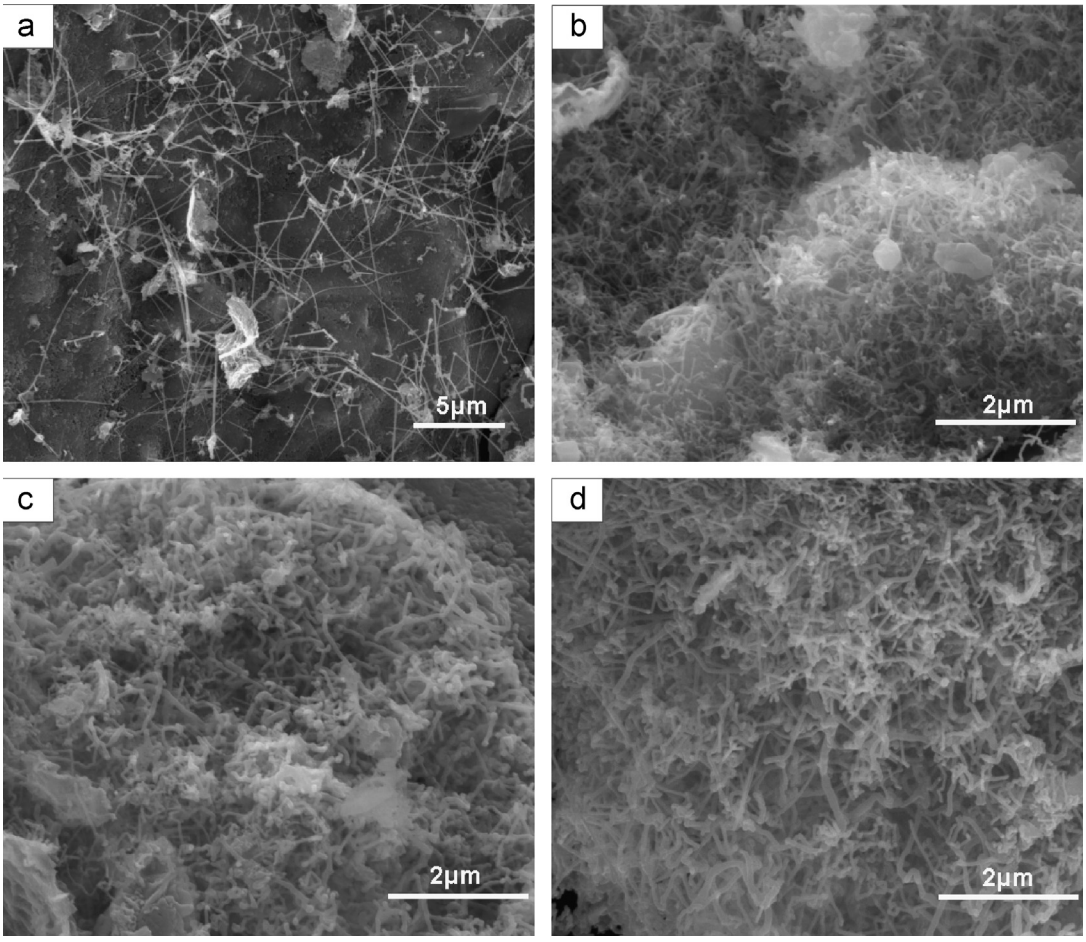

Fig. 4. SEM micrographs of samples with an Si:graphite ratio of 1:2 heat-treated for 3 h at (a) 1250 °C, (b) 1300 °C, (c) 1350 °C, and (d) 1400 °C.

The XRD patterns given in Figs. 1 and 2 were also used to calculate the relative proportions of the resultant SiC nanowires. The effect of temperature of heat treatment on the relative content is shown in Table 1. The results indicated that the relative content of SiC in the products gradually increased with increased calcining temperature, and up to 12% w/w at 1400 °C. As expected, the increase in temperature caused a continuous increase in the relative content of obtained SiC nanowires. Furthermore, Table 2 shows that the formation of SiC did not increase monotonically with prolonged heat treatment time. The relative content of SiC in the product reached its maximum value when the sample was heated at 1400 °C for 3 h.

Another important parameter with the molten salt synthesis is the Si/graphite ratio. An excess of graphite is normally used in SiC nanowire synthesis especially when it is deposited on the graphite's surface. An excess of graphite was found to be effective in increasing the contact area between Si and graphite particles and therefore accelerating the SiC synthesis. As can be seen in Fig. 3, the relative intensities of β-SiC peaks as well as the amounts of β-SiC created in samples with Si/graphite ratios of 1:1, 1:3, and 1:4 were almost equal. When the Si/graphite ratio was 1:2, the β-SiC peaks were slightly higher than the others. It can be seen that the Si/graphite ratio did not affect the formation of SiC in any significant way beyond increasing the contact area. Therefore the following discussion will focus on samples with Si/graphite ratio of 1:2.

3.2. Microstructural analysis

Fig. 4 is an SEM image of the as-prepared β-SiC nanowires growing on the surface of the graphite: the SiC nanowires obtained at 1250 °C were small in number. However, an increase in heat treatment temperature to 1300 °C significantly changed the amount of SiC nanowires as shown in Fig. 4(b). It is seen that there is a thick layer of β-SiC nanowires on the graphite surface, which indicated that the formation of SiC nanowires was by growth on some random facet of the graphite surface. Fig. 4(c) and (d) reveals that increase in heat treatment temperature to 1350 °C and 1400 °C did not change the shape of the nanowires, and only some areas of the nanowires became thicker and longer. It is believed that the heat treatment at temperatures as high as 1400 °C promoted growth of SiC nanowires. Support for the above conclusion is also found in Table 1.

The effect of holding time at 1350 °C on microstructure of SiC nanowires is presented in Fig. 5(a) and (b). When compared to a sample treated for 1 h, it can be noted that prolonged holding time significantly increased the length of nanowires and the shape became slightly straighter. Fig. 5 provided additional support for the conclusion that prolonged holding time at 1350 °C promoted nanowire growth.

The magnified SEM image, Fig. 6(a), further shows that the lengths of the nanowires was approximately 1–10 μm, and their diameter approximately 10–50 nm. Fig. 6(b) and (c) shows TEM images of nanowires produced from samples heated for 3 h in NaF–NaCl at 1350 °C, along with the SAED pattern of the latter (Fig. 6(b) inset). The diffraction rings in the SAED pattern also matched the (111), (220), and (311) diffraction planes of β-SiC.

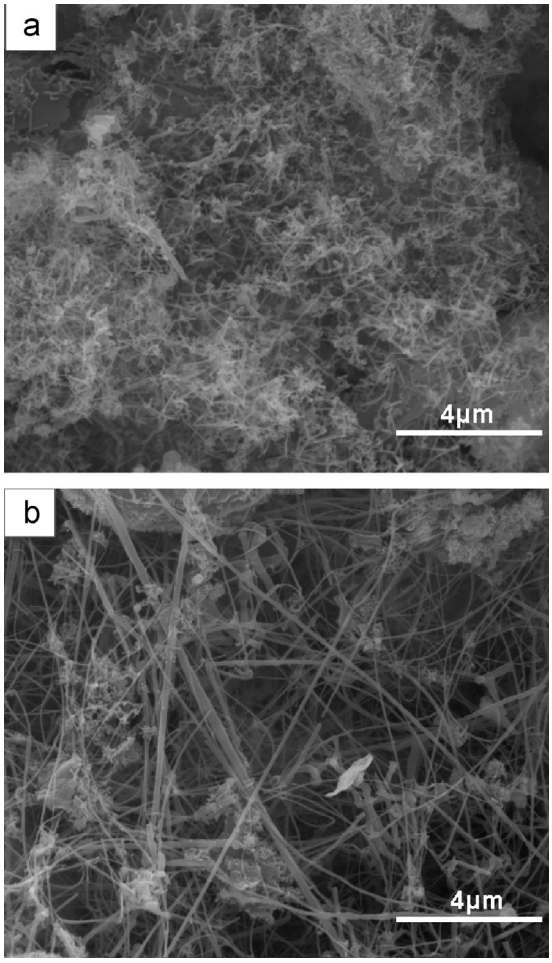

Fig. 5. SEM micrographs of samples with an Si/graphite ratio of 1:2 heat-treated at 1350 °C for different holding times (a) 1 h, and (b) 5 h.

This, along with the XRD results shown in Figs. 1–3, confirmed that for the main formation of β-SiC nanowires. Fig. 6(c) shows the corresponding HRTEM image of an individual SiC nanowire, which indicated a single crystalline structure for the nanowire. Three β-SiC peaks at 35.7, 60.0, and 71.8 were observed, corresponding to the diffractions from SiC's (111), (220), and (311) planes respectively, indicating the formation of β-SiC (JCPDS Card no.75-0254). The spacing between adjacent lattice planes was 0.25 nm, corresponding to the (111) plane of β-SiC, which indicated that the preferred growth direction of nanowires was perpendicular to (111).

3.3. Zeta potential vs pH

Fig. 7 shows the change in zeta potential with pH of the modified graphite, the Si/graphite ratios: 1:4, 1:3, 1:2, and 1:1 are compared with the unmodified graphite. The zeta potential of graphite is around zero, and its potential value was almost zero [24]. When the molar ratio of silicon/graphite was 1:4, because of the higher graphite content and fewer SiC nanowires being generated, the sample showed that its tendency lay close to the zeta potential of graphite as shown in Fig. 7. However, as the molar ratio of silicon/graphite further increased, the generated SiC

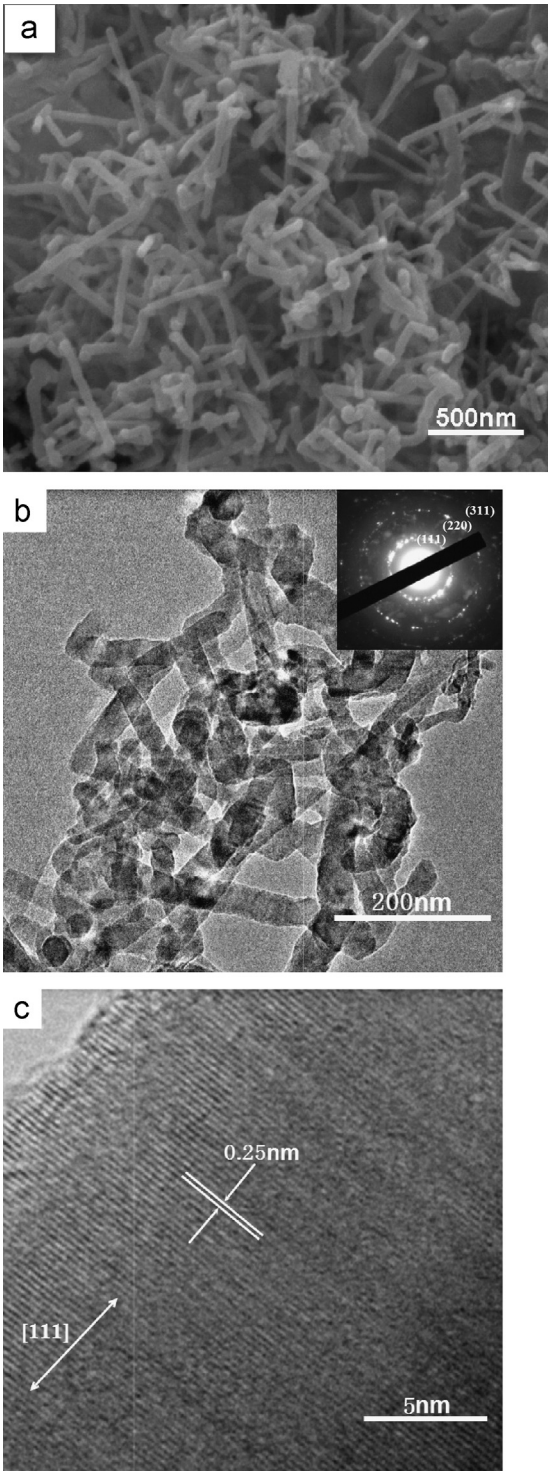

Fig. 6. SEM micrograph of sample with an Si/graphite ratio of 1:2 heat-treated for 3 h at 1350 °C (a), TEM micrograph (b), corresponding SAED pattern (inset) and HRTEM image of an individual SiC nanowire (c).

nanowires in relevant samples also increased. So it was found that the surface morphology of the modified graphite has been completely changed at this moment, which, to some extent, explained the relationship between zeta potential and pH value of SiC in water [30–35]. The high positive potential at low pH provided a repulsive barrier between powder particles to decrease

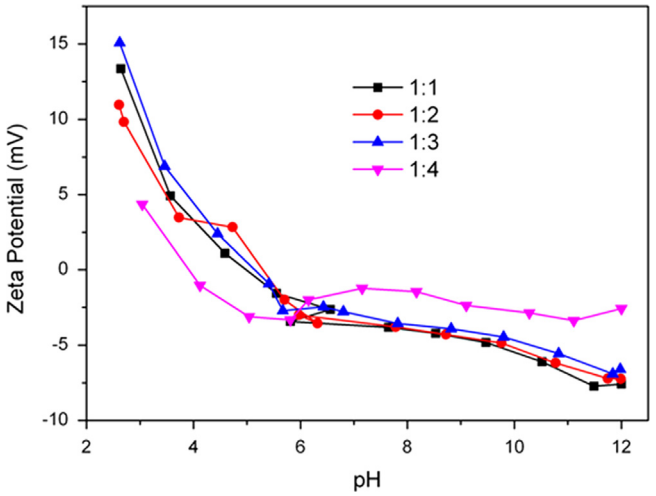

Fig. 7. Zeta potential as a function of pH for a graphite surface modified with SiC nanowires.

the slurry viscosity: the viscosity increase intrinsically depended on the particle size distribution of fine powders, their morphology, density, type, concentration of dispersing agents, *etc* [36,37]. In our case, the electrokinetic behavior of coated SiC nanowires is shown in Fig. 7. The coated graphite showed a higher zeta potential compared to the uncoated graphite, which was associated with its wettability in water. The coating changed the graphite's electrokinetic properties and viscosity: a low viscosity is favorable for castable flow behavior. Also when such coatings are developed on graphite surfaces in an acidic atmosphere, its hydrophilicity was further improved.

3.4. Oxidation resistance of SiC nanowires

The oxidation resistance of all the treated samples, including as-received ones, was evaluated by DSC/TG measurement (Fig. 8). The samples were heated from room temperature to 1200 °C in a static air atmosphere at a rate of 10 °C/min. According to the DSC curves, it was found that there was an exothermic peak on the treated samples with Si/graphite ratios of 1:2, 1:3, and 1:4 from 650 °C to 850 °C, and flake graphite began to oxidize at about 650 °C then a high exothermic peak appeared between 650 °C and 1000 °C. As for those treated samples, some results can be seen correspondingly from the presented TG curves, when the graphite content was higher, part of the graphite in the treated samples was oxidized firstly at between 650 °C and 850 °C: the graphite then began to oxidize at 650 °C and its mass reduced gradually, while those untreated graphite samples were fully oxidized. Because a small amount of SiC nanowires were generated in the treated samples, those SiC nanowires were the first to be oxidized, and the generation of SiO_2 from oxidization increased with the mass available from 850 °C to 1100 °C [38]. The graphite was then oxidized along with an accompanying mass loss. It can be seen from the experiment that SiC nanowires formed on the graphite surface acted as an anti-oxidant to a certain extent, the SiO_2 formed on the graphite surface in the process of oxidation had reduced the oxidation rate of graphite, and as they increased in quantity, they further prevented the inner graphite from oxidation.

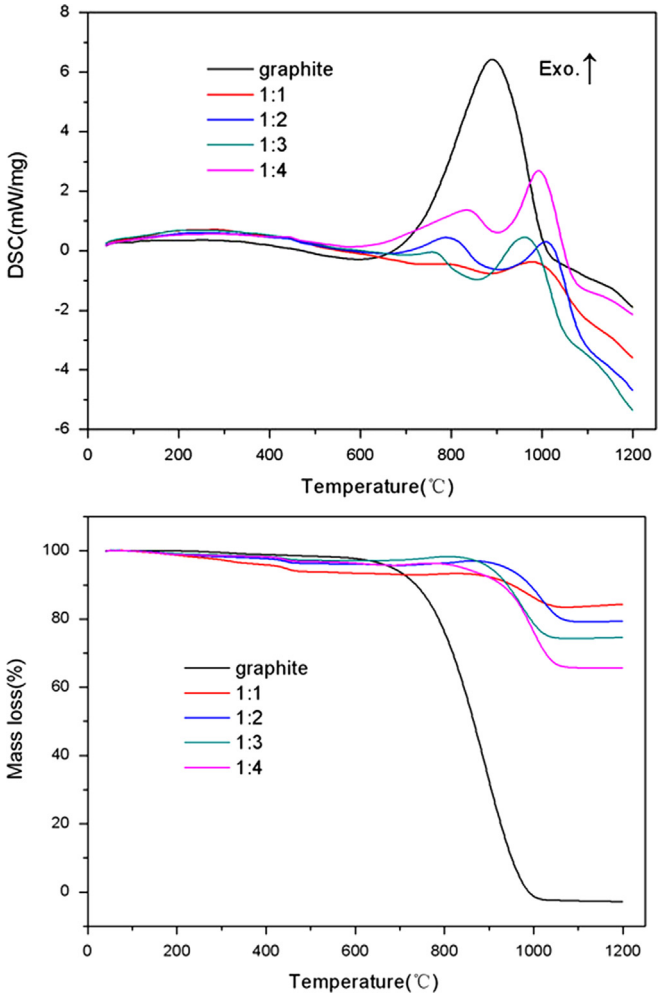

Fig. 8. DSC and TG curves of samples heat-treated at 1350 °C for 3 h with different Si/graphite ratios.

4. Conclusions

Silicon carbide nanowires were synthesized by partially reacting with silicon powders in NaF–NaCl based salts on graphite surfaces: their preferred growth direction was perpendicular to (111). The nanowires were approximately 10–50 nm in diameter, with variable lengths. Heat treatment at higher temperatures, such as 1400 °C, and prolonged holding times promoted nanowire growth. It was found that the surface features of modified graphite had been completely changed. The SiC whiskers that had formed on the graphite's surface acted as an anti-oxidant to a certain extent and, as such, prevented the inner graphite from oxidation.

Acknowledgments

This work is financially supported by the Natural Science Foundation of China (Grant no. 51074118) and National Key Basic Research Program of China (973) (No. 2012CB722702).

References

[1] J.K. Ye, S.W. Zhang, W.E. Lee, Novel low temperature synthesis and characterisation of hollow silicon carbide spheres, Microporous and Mesoporous Materials 152 (2012) 25–30.
[2] K. Senthil, K. Yong, Enhanced field emission from density-controlled SiC nanowires, Materials Chemistry and Physics 112 (2008) 88–93.
[3] Y.F. Chen, X.Z. Liu, X.W. Deng, Factors affecting the growth of SiC nano-whiskers, Journal of Materials Science and Technology 26 (11) (2010) 1041–1046.
[4] J.J. Chen, Q. Shi, W.H. Tang, Field emission performance of SiC nanowires directly grown on graphite substrate, Materials Chemistry and Physics 126 (2011) 655–659.
[5] Y.J. Wu, J.S. Wu, W. Qin, D. Xu, Z.X. Yang, Y.F. Zhang, Synthesis of h-SiC nanowhiskers by high temperature evaporation of solid reactants, Materials Letters 58 (2004) 2295–2298.
[6] W. Xie, G. Mobus, S.W. Zhang, Molten salt synthesis of silicon carbide nanorods using carbon nanotubes as templates, Journal of Materials Chemistry 21 (2011) 18325–18330.
[7] J.W. Liu, D.Y. Zhong, F.Q. Xie, M. Sun, E.G. Wang, W.X. Liu, Synthesis of SiC nanofibers by annealing carbon nanotubes covered with Si, Chemical Physics Letters 348 (2001) 357–360.
[8] C.L. Yeh, Y.D. Chen, Direct formation of titanium carbonitrides by SHS in nitrogen, Ceramics International 31 (5) (2005) 719–729.
[9] W. Yang, H. Araki, S. Thaveethavorn, H. Suzuki, T. Noda, In situ synthesis and characterization of pure SiC nanowires on silicon wafer, Applied Surface Science 241 (2005) 236–406.
[10] B. Babic, D. Bucevac, A. Radosavljevic-Mihajlovic, A. Dosen, J. Zagorac, J. Pantic, B. Matovic, New manufacturing process for nanometric SiC, Journal of the European Ceramic Society 32 (2012) 1901–1906.
[11] H.J. Li, Z.J. Li, A.L. Meng, K.Z. Li, X.N. Zhang, Y.P. Xu, SiC nanowire networks, Journal of Alloys and Compounds 352 (2003) 279–282.
[12] Y. Baek, Y. Ryu, K. Yong, Structural characterization of β-SiC nanowires synthesized by direct heating method, Materials Science and Engineering C 26 (2006) 805–808.
[13] W.S. Shi, Y.F. Zheng, H.Y. Peng, N. Wang, C.S. Lee, S.T. Lee, Laser ablation synthesis and optical characterization of silicon carbide nanowires, Journal of the American Ceramic Society 83 (2000) 3228–3230.
[14] J.Z. Guo, Y. Zuo, Z.J. Li, W.D. Gao, J.L. Zhang, Preparation of SiC nanowires with fins by chemical vapor deposition, Physica E 39 (2007) 262–266.
[15] Z.S. Wu, S.Z. Deng, N.S. Xu, J. Chen, J. Zhou, J. Chen, Needle-shaped silicon carbide nanowires: synthesis and field electron emission properties, Applied Physics Letters 80 (2002) 3829–3831.
[16] Y.B. Li, S.S. Xie, W.Y. Zhou, L.J. Ci, Y.S. Bando, Cone-shaped hexagonal 6H–SiC nanorods, Chemical Physics Letters 356 (2002) 325–330.
[17] X.W. Du, X. Zhao, S.L. Jia, Y.W. Lu, J.J. Li, N.Q. Zhao, Direct synthesis of SiC nanowires by multiple reaction VS growth, Materials Science and Engineering B 136 (2007) 72–77.
[18] L.P. Xin, Q. Shi, J.J. Chen, W.H. Tang, N.Y. Wang, Y. Liu, Y.X. Lin, Morphological evolution of one-dimensional SiC nanomaterials controlled by sol–gel carbothermal reduction, Materials Characterization 65 (2012) 55–61.
[19] X. Liu, S. Zhang, Low-temperature preparation of titanium carbide coatings on graphite flakes from molten salts, Journal of the American Ceramic Society 91 (2) (2008) 667–670.
[20] S. Yilmaz, Y. Kutmen-Kalpakli, E. Yilmaz, Synthesis and characterization of boehmitic alumina coated graphite by sol–gel method, Ceramics International 35 (2009) 2029–2034.
[21] Q. Li, G.Z. Zeng, W.F. Zhao, G.H. Chen, Preparation and characterization of nickel-coated graphite nanosheets, Synthetic Metals 160 (2010) 200–202.
[22] S. Zhang, W.E. Lee, Influence of additives on corrosion resistance and corroded microstructures of Mg–O refractories, Journal of the European Ceramic Society 21 (2001) 2393–2405.
[23] D.D. Jayaseelan, S.W. Zhang, S.B. Hashimoto, W.E. Lee, Template formation of magnesium aluminate ($MgAl_2O_4$) spinel microplatelets in molten salt, Journal of the European Ceramic Society 27 (2007) 4745–4749.
[24] A. Saberi, F. Golestani-Fard, M. Willert-Porada, R. Simon, T. Gerdes, H. Sarpoolaky, Improving the quality of nanocrystalline $MgAl_2O_4$ spinel

coating on graphite by a prior oxidation treatment on the graphite surface, Journal of the European Ceramic Society 28 (2008) 2011–2017.
[25] J. Ding, C.J. Deng, W.J. Yuan, H.X. Zhu, J. Li, The synthesis of titanium nitride whiskers on the surface of graphite by molten salt media, Ceramics International 39 (2013) 2995–3000.
[26] J.K. Ye, S.W. Zhang, W.E. Lee, Molten salt synthesis and characterization of SiC coated carbon black particles for refractory castable applications, Journal of the European Ceramic Society 33 (2013) 2023–2029.
[27] W. Xie, Z. Mirza, G. Möbus, S. Zhang, Novel synthesis and characterization of high quality silicon carbide coatings on carbon fibers, Journal of the American Ceramic Society 95 (6) (2012) 1878–1882.
[28] R.L. Snyder, The use of reference intensity ratios in X-ray quantitative analysis, Powder Diffraction 7 (4) (1992) 186–193.
[29] J.M. Qian, J.P. Wang, G.J. Qiao, Z.H. Jin, Preparation of porous SiC ceramic with a woodlike microstructure by sol–gel and carbothermal reduction processing, Journal of the European Ceramic Society 24 (2004) 3251–3259.
[30] R. Wasche, M. Naito, Vincent A. Hackley, Experimental study on zeta potential and streaming potential of advanced ceramic powders, Powder Technology 123 (2002) 275–281.
[31] M. Castellote, I. Llorente, C. Andrade, Influence of the composition of the binder and the carbonation on the zeta potential values of hardened cementitious materials, Cement and Concrete Research 36 (2006) 1915–1921.
[32] A. Wiacek, Investigations of DPPC effect on Al_2O_3 particles in the presence of (phospho) lipases by the zeta potential and effective diameter measurements, Applied Surface Science 257 (2011) 4495–4504.
[33] P. Leroy, C. Tournassat, Mohamed Bizi, Influence of surface conductivity on the apparent zeta potential of TiO_2 nanoparticles, Journal of Colloid and Interface Science 356 (2011) 442–453.
[34] H. Simunkova, P. Pessenda-Garcia, J. Wosik, P. Angerer, H. Kronberger, G. Nauer, The fundamentals of nano- and submicro-scaled ceramic particles incorporation into electrodeposited nickel layers: zeta potential measurements, Surface and Coatings Technology 203 (2009) 1806–1814.
[35] Y. Zeng, A. Zimmermann, F. Aldinger, D.L. Jiang, Effect of organic additives on the zeta potential of PLZST and rheological properties of PLZST slurries, Journal of the European Ceramic Society 28 (2008) 2597–2604.
[36] S. Mukhopadhyay, S. Dutta, Comparison of solid state and sol–gel derived calcium aluminate coated graphite and characterization of prepared refractory composite, Ceramics International 38 (2012) 4997–5006.
[37] A.R. Studart, V.C. Pandolfelli, J. Gallo, Dispersants for high alumina castables, American Ceramic Society Bulletin 81 (2002) 36–44.
[38] Q.S. Zhu, X.L. Qiu, C.W. Ma, Oxidation resistant SiC coating for graphite materials, Carbon 37 (1999) 1475–1484.